Liquid Crystals
Publication details, including instructions for authors and subscription information:
http://www.informaworld.com/smpp/title~content=t713926090

Synthesis and mesomorphic behaviour of heterocycle-based liquid crystals containing 1,3,4-oxadiazole/thiadiazole and thiophene units

Jie Han[a]; Juan-Yu Wang[a]; Feng-Yan Zhang[a]; Li-Rong Zhu[a]; Mei-Li Pang[a]; Ji-Ben Meng[a]
[a] Department of Chemistry, Nankai University, Tianjin 300071, P.R. China

To cite this Article Han, Jie , Wang, Juan-Yu , Zhang, Feng-Yan , Zhu, Li-Rong , Pang, Mei-Li and Meng, Ji-Ben(2008) 'Synthesis and mesomorphic behaviour of heterocycle-based liquid crystals containing 1,3,4-oxadiazole/thiadiazole and thiophene units', Liquid Crystals, 35: 10, 1205 — 1214
To link to this Article: DOI: 10.1080/02678290802444129
URL: http://dx.doi.org/10.1080/02678290802444129

Liquid Crystals,
Vol. 35, No. 10, October 2008, 1205–1214

Taylor & Francis
Taylor & Francis Group

Synthesis and mesomorphic behaviour of heterocycle-based liquid crystals containing 1,3,4-oxadiazole/thiadiazole and thiophene units

Jie Han*, Juan-Yu Wang, Feng-Yan Zhang, Li-Rong Zhu, Mei-Li Pang and Ji-Ben Meng

Department of Chemistry, Nankai University, Tianjin 300071, P.R. China

(Received 11 August 2008; final form 1 September 2008)

A new class of thiophene-based 1,3,4-oxadiazole derivatives (***n*-OXD-R**) and the corresponding 1,3,4-thiadiazole derivatives (***n*-THD-R**) was synthesised and characterised by means of ^{1}H NMR, ^{13}C NMR, MS and HRMS techniques. Liquid crystal properties were investigated by differential scanning calorimetry, polarising optical microscopy and variable temperature X-ray diffraction measurements. All the 1,3,4-thiadiazole compounds (***n*-THD-R**) exhibited enantiotropic mesophases (smectic A, smectic C and nematic phases) with wide mesomorphic temperature ranges (68.5–109.5°C). In contrast, only the oxadiazole compounds **8-OXD-Cl**, **9-OXD-Cl** and **10-OXD-Cl**, bearing electron-withdrawing terminal group and longer alkoxy chain, displayed an enantiotropic smectic A phase with narrow mesomorphic temperature ranges (4.1–10.9°C). The effects of central heterocyclic rings, the terminal groups and the length of the terminal alkoxy on the mesomorphic behaviour are discussed.

Keywords: 1,3,4-oxadiazole derivative; 1,3,4-thiadiazole derivative; thiophene liquid crystals; synthesis

1. Introduction

Selection of a mesogenic core unit, terminal groups and suitable length of one or more flexible chains is the common method to design new thermotropic liquid crystals (*1*). Among the reported rod-like mesogens, a *para*-substituted phenyl ring often serves as a major core unit, which ensures that the molecules have structural linearity and large molecular polarisability, and consequently that they exhibit liquid crystalline behaviour (*2*). Recently, there has been a continuing interest in the study of heterocyclic-based liquid crystal compounds owing to the great variety of their structures (*3*). Moreover, the nonlinearity of heterocyclic liquid crystals may result in lower melting points than the 1,4-phenylene counterparts owing to the reduced packing efficiency of the molecules (*4*). Among the heterocyclic mesogens, much attention has paid to 2,5-disubstituted 1,3,4-oxadiazoles/1,3,4- thiadiazoles owing to their rich mesophases and good thermal stability. In addition, this type of liquid crystal emits strong fluorescent light with high quantum yield and may potentially be used as functional materials (*5, 6*). Thiophene, another type of five-membered ring, is also used as a core to devise mesogenic compounds because thiophene-based liquid crystals have many merits, such as low melting point and viscosity, large optical anisotropy and fast switching times (*7*).

In this paper, we report the combination of structural characteristics of 1,3,4-oxadiazole/thiadiazole and thiophene rings and the synthesis of a new class of 2-(4-alkoxyphenyl)-5-(5-substituted thien-2-yl)-1,3,4-oxadiazoles and their corresponding 1,3,4-thiadiazole analogues. The synthetic route and the reaction conditions are shown in Scheme 1. The liquid crystalline properties of these new compounds were investigated in detail. The relationship between their molecular structures and liquid crystal properties is discussed.

2. Results and discussion

Synthesis and characterisation

1,3,4-Oxadiazole derivatives can be obtained efficiently by several approaches (*8*). In this study, compounds ***n*-OXD-R** were prepared in good yields (70–80%) by the standard procedures (*8a*), which were carried out by boiling the appropriate solution of *N*,*N*′-diaryl hydrazides (**i**–**viii**) in thionyl chloride. 1,3,4-Thiadiazole derivatives are often prepared by sulfuration of 1,4-dicarbonyl precursors with P_2S_5 or Lawesson's reagent in anhydrous hydrocarbon solvents at high temperature (*9*). In addition, microwave-assisted synthesis has also been used as an efficient method to prepare 1,3,4-thiadiazole derivatives due to its low-cost, operational simplicity, relatively shorter reaction time and sometimes solvent-free reaction conditions (*10*). In this study, the 1,3,4-thiadiazoles ***n*-OXD-Cl** (n=5, 6, 7, 8) were prepared under microwave irradiation and solvent conditions; indeed, the procedures have many merits, such as short reaction time (only around 120 s),

*Corresponding author. Email: hanjie@nankai.edu.cn

ISSN 0267-8292 print/ISSN 1366-5855 online

DOI: 10.1080/02678290802444129
http://www.informaworld.com

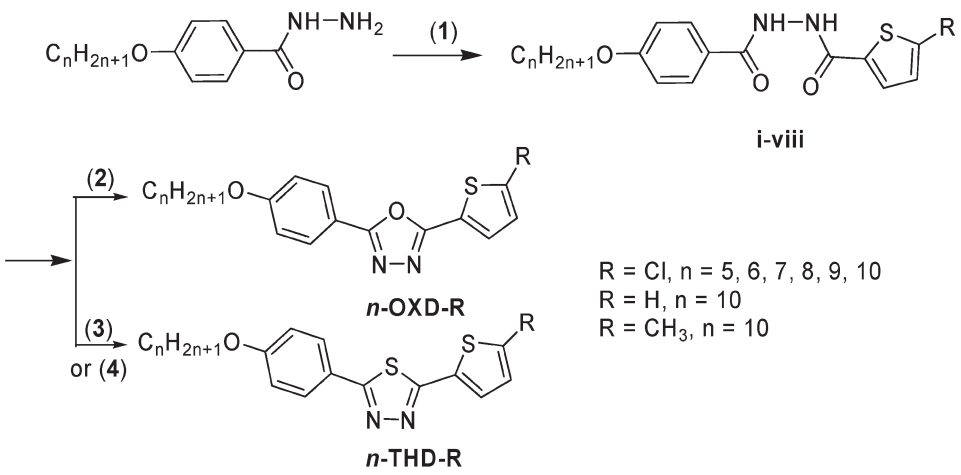

Scheme 1. Reagents and conditions: (**1**) 5-chloro-2-thiophenecarbonyl chloride, stirred in pyridine for 4 h at room temperature, then heated to 80°C for 0.5 h, 80–90%; (**2**) $SOCl_2$ (10 equiv.), reflux, 7 h, 70–80%; (**3**) Lawesson's reagent (1.1 equiv.), microwave irradiation, 120 s, 25–50%; (**4**) Lawesson's reagent (1.1 equiv.), refluxed in toluene (10 h), 62–75%.

simple workup and environment-friendly conditions, but the yields are relatively low or moderate (25–50%) because it is difficult to control precisely the microwave irradiation time. We found that the microwave irradiation time was a key factor in determining the yields. The reaction did not occur at all with inadequate irradiation time, whereas prolonged irradiation resulted in decomposition or combustion of the reaction products. In contrast, compounds **9-OXD-Cl** and **10-OXD-R** (R = Cl, H, CH_3) were obtained in moderate to good yields (62–75%) by boiling the corresponding intermediates in toluene for about 10 h.

Mesophases characterisation and thermal properties

The liquid crystal properties of all compounds ***n*-OXD-R** and ***n*-THD-R** were investigated by means of differential scanning calorimetry (DSC), variable temperature X-ray diffraction (VXRD) and polarising optical microscopy (POM). The mesophases were identified according to the classification system reported by Kumar (*11*) and Dierking (*12*). For the 1,3,4-oxadiazoles, only **8-OXD-Cl**, **9-OXD-Cl** and **10-OXD-Cl** exhibited an enantiotropic smectic A (SmA) phase with narrow mesomorphic temperature ranges (4.1°C for **8-OXD-Cl**, 7.4°C for **9-OXD-Cl** and 10.9°C for **10-OXD-Cl** during the heating process). As an example, Figure 1(a) depicts a characteristic fan-shaped texture of the SmA phase on cooling from the isotropic melt of **10-OXD-Cl** at 103.7°C. In contrast to the oxadiazoles, all the thiadiazoles ***n*-THD-R** exhibited stable liquid crystalline behaviour with wide mesomorphic temperature ranges. For ***n*-THD-Cl** (n = 5–10) and **10-THD-H**, independent of the length of the alkoxy chain or the type of terminal group, they all displayed an enantiotropic SmA mesophase, which was identified by the typical polygonal (Figure 1(b)), focal conic (Figure 1(c)) or bâtonnets textures (Figure 1(d)), all of which are characteristic of SmA phases. In contrast, compound **10-THD-CH_3** exhibited enantiotropic nematic and smectic C (SmC) phases. Upon cooling the isotropic melt of **10-THD-CH_3**, typical nematic droplets (Figure 1(e)) formed at first, then these droplets joined together to give the nematic threaded texture. Upon further cooling, the nematic phase resulted in the formation of SmC phase, as can be seen in Figure 1(f).

Both the oxadiazoles ***n*-OXD-R** and the thiadiazoles ***n*-THD-R** were studied by DSC. The phase transition temperatures and enthalpies of these compounds are summarised in Table 1. All the DSC results are consistent with the respective observations of textures using POM. As representative examples, only the DSC thermograms of **8-OXD-Cl**, **8-THD-Cl** and **10-THD-CH_3** are shown in the Figure 2. For the oxadiazole **8-OXD-Cl**, during the heating run rich crystal-to-crystal transitions were observed, preceding the melting peak at 103.7°C, the highest temperature weak peak at 107.8°C should be attributed to the SmA–isotropic transition. All these transition temperature ranges are very narrow and can not be separated effectively at a heating rate of 5°C min^{-1}. Upon cooling, the DSC thermogram of **8-OXD-Cl** is relatively simple, although there is also a crystal-to-crystal transition at 60.5°C. The mesomorphic temperature range (3.4°C) during the cooling process is comparable to that (4.1°C) of the heating cycle. As can be seen in Figure 2(b), the DSC thermograms of the thiadiazole **8-THD-Cl** exhibit two clear-cut transitions both on heating and on cooling. In the heating

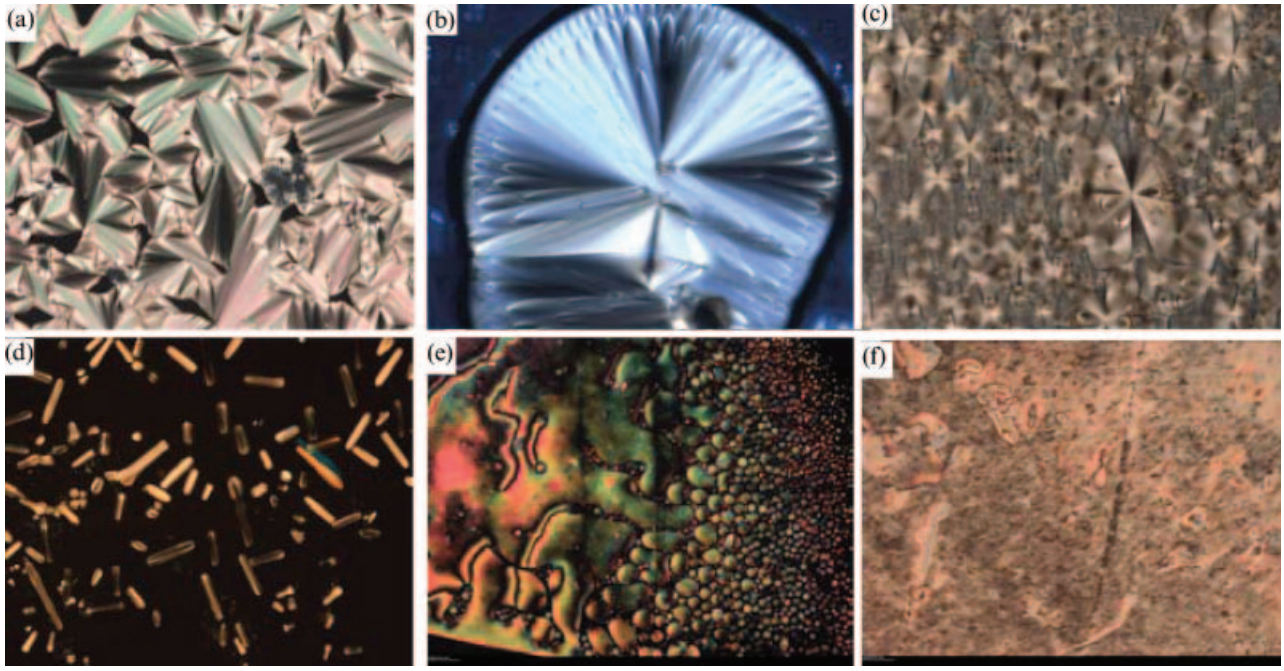

Figure 1. Photomicrographs of: (a) fan-shaped and focal conic texture of SmA phase of **10-OXD-Cl** at 103.7°C on cooling (200×); (b) polygonal texture of SmA phase of **5-THD-Cl** at 213.9°C on cooling (500×); (c) focal conic texture of SmA phase of **9-THD-Cl** at 214.8°C on heating (200×); (d) bâtonnets texture of SmA phase of **10-THD-Cl** at 213.9°C on cooling (200×); (e) nematic phase of **10-THD-CH$_3$** at 162.1°C on cooling (200×); (f) SmC phase of **10-THD-CH$_3$** at 108.5°C on cooling (200×).

thermogram, the larger peak area at 121.6°C is due to the crystal–SmA phase transition, and the relatively small peak area at 218.4°C is due to the SmA–isotropic transition. The two transitions in the cooling thermogram may also be reasonably assigned as the isotropic–SmA (215.1°C) and SmA–crystal transitions, respectively. In contrast, the DSC thermograms (Figure 2(c)) of **10-THD-CH$_3$** show three clear-cut peaks both in the heating and cooling runs. The largest peak area at 106.3°C is attributed to the melting process, and the two small peak areas at 124.9°C and 160.4°C are due to the SmC–nematic phases and isotropisation transitions, respectively. The identity of a nematic mesophase for **10-THD-CH$_3$** is also supported by the transition enthalpy of the clearing point. The isotropisation enthalpy of 1.62 kJ mol^{-1} is typical for a nematic–isotropic transition (typically 1–2 kJ mol^{-1}) (*13*).

The phase transitions of compound **8-THD-Cl** were further confirmed by in-situ VXRD measurements. The diffractogram shown in Figure 3 reveals the phase transitions from the crystal to fluid smectic phase and finally to the isotropic phase. At room temperature (30°C), the diffractogram shows a strongest diffraction peak (2θ=3.75°, d=23.6 Å) and three consecutive low-angle diffraction peaks (2θ=7.50°, 11.25° and 15°). The 2θ values of three consecutive low-angle diffraction peaks arranged in a periodic order, indicating the lamellar arrangement of the molecules. As the temperature is increased to 140°C, the diffractogram shows a very strong peak (2θ=3.45°, d_{100}=25.6 Å) and a weak peak (2θ=6.90°, d_{200}=12.8 Å) derived from the second-order reflection in the small-angle region. The 2θ value of the strong diffraction peak shifted from 3.75° to 3.45° when the temperature increased from 30°C to 140°C; this peak shift is due to the formation of the SmA phase. When the temperature increased to 230°C, the strong diffraction peak and the weak peaks in the small region disappeared completely, indicating the formation of the isotropic liquid of **8-THD-Cl**.

Figure 4 shows thermogravimetric analysis curves of the selected compounds **8-OXD-Cl**, **8-THD-Cl** and **8-THD-H**, which show that all these solid samples exhibited no weight loss in the temperature range 25–300°C. All of them started to lose weight at 309–340°C in a single step with the whole process completed at about 380°C, which reveals that all these compounds possess excellent thermal stability. Thus, all the phase transition temperatures of these liquid crystal materials are much lower than their thermal decomposition temperatures (320.5°C for **8-OXD-Cl**, 309.8°C for **8-THD-Cl** and 340.3°C for **8-THD-H**, respectively).

Table 1. Phase transition temperatures (°C) and enthalpies (kJ mol^{-1}, in parentheses) of ***n*-OXD-R** and ***n*-THD-R** on the first heating and cooling runs at a scan rate of 5°C min^{-1}.

Compound	Phase transitions[a]
5-OXD-Cl	Cr 115.5 (30.25) I
	I 100.7 (−29.51) Cr
6-OXD-Cl	Cr 98.0 (26.99) I
	I 95.2 (−15.97) Cr_1 71.3 (−7.22) Cr_2
7-OXD-Cl	Cr 87.2 (22.49) I
	I 79.7 (−8.48) Cr_1 64.1 (−11.52) Cr_2
8-OXD-Cl	Cr_1 94.6 Cr_2 99.3 Cr_3 103.7 SmA 107.8 (40.19[b]) I
	I 102.5 (−4.12) SmA 99.1 (−14.27) Cr_4 60.5 (−8.05) Cr_5
9-OXD-Cl	Cr_1 96.6 (21.12) Cr_2 100.3 (8.55) SmA 107.9 (3.04) I
	I 104.6 (−5.04) SmA 97.4 (−11.81) Cr_3 56.8 (−10.74) Cr_4
10-OXD-Cl	Cr_1 95.0 (27.53) Cr_2 97.4 (9.98) SmA 108.3 (3.83) I
	I 104.6 (−5.04) SmA 97.4 (−11.81) Cr_3 56.8 (−10.74) Cr_4
10-OXD-H	Cr 95.4 (41.43) I
	I 65.2 (−38.12) Cr
10-OXD-CH_3	Cr 105.5 (43.96) I
	I 65.5 (−36.01) Cr
5-THD-Cl	Cr 148.8 (29.17) SmA 217.3 (7.11) I
	I 218.0 (−7.00) SmA 120.8 (−23.85) Cr
6-THD-Cl	Cr 132.4 (25.45) SmA 219.3 (7.84) I
	I 215.5 (−8.30) SmA 114.6 (−24.81) Cr
7-THD-Cl	Cr 114.8 (22.86) SmA 213.0 (0.49) I
	I 206.7 (−1.92) SmA 98.0 (−20.57) Cr
8-THD-Cl	Cr 121.6 (28.89) SmA 218.4 (8.68) I
	I 215.1 (−8.41) SmA 99.8 (−26.64) Cr
9-THD-Cl	Cr 104.6 (34.23) SmA 214.1 (8.90) I
	I 212.3 (−8.46) SmA 91.8 (−32.99) Cr
10-THD-Cl	Cr_1 112.1 (35.94) SmA 213.1 (8.57) I
	I 208.6 (−7.09) SmA 94.7 (−4.34) Cr_2 91.7 (−26.70) Cr_3
10-THD-H	Cr_1 71.3 (0.98) Cr_2 101.3 (24.44) SmA 118.5 (5.52) I
	I 117.1 (−5.72) SmA 84.4 (−24.64) Cr_3
10-THD-CH_3	Cr 106.3 (39.78) SmC 124.9 (0.47) N 160.4 (1.62) I
	I 159.1 (−1.40) N 123.3 (−0.58) SmC 92.2 (−37.06) Cr

[a]Cr_n=crystal phase; N=Nematic phase; SmA=smectic A phase; SmC=smectic C phase; I=isotropic liquid. [b]The total enthalpy of the Cr_1–I transition cannot being integrated individually.

Relationship between the structure and liquid crystal properties

As seen in Table 1, most of the 1,3,4-oxadiazoles (***n*-OXD-R**) are non-mesogenic, whereas all the corresponding 1,3,4-thiadiazoles (***n*-THD-R**) exhibited stable mesophases with wide temperature ranges, indicating that the liquid crystal properties were affected greatly by the central heterocyclic rings. According the single crystal structures of 2,5-disubstituted 1,3,4-oxadiazoles and 1,3,4-thiadiazoles reported in the literature (*14*), it is known that the 1,3,4-thiadiazole moiety apparently favours formation of rod-like molecules with large bent angles (ca. 167–169°), as shown in Scheme 2, which enables more efficient and closer packing of molecules in the respective mesophases, compared with the bent-shaped 1,3,4-oxadiazole analogues (bent angle ca. 134–135°). Consequently, the linearity of the molecule generates a larger dipole moment, which could readily account for the result that the 1,3,4-thiadiazole derivatives ***n*-THD-R** exhibited wider mesomorphic temperature ranges with higher clearing points, compared with that of the 1,3,4-oxadiazoles ***n*-OXD-R**.

Parra *et al.* (*15*) compared the effect of 1,3,4-oxadiazole and 1,3,4-thiadiazole rings on liquid crystalline properties by means of semi-empirical calculations. They studied the rotational barrier around the C (heterocyclic)–N (imine) bond of model compounds, 5-(4-ethoxy)-phenyl-2-(2-hydroxyl-4-methoxy)- benzylideneamino-1,3,4-oxadiazole/thiadiazole, and found that the rotational barrier for the 1,3,4-thiadiazole compound is much higher than that of the oxadiazole compound (*15*). According to Parra's results, we may conclude that the rotational barrier around the C (heterocyclic)–C (thienyl) bond for ***n*-THD-R** may be also higher than that of the corresponding bond for ***n*-OXD-R**. The higher rotational barrier may be helpful to the stable molecular packing with rod-like shape, and consequently facilitate the formation of mesophases in the 1,3,4-thiadiazole derivatives ***n*-THD-R**. In contrast, the lower rotational barrier in the 1,3,4-oxadiazole

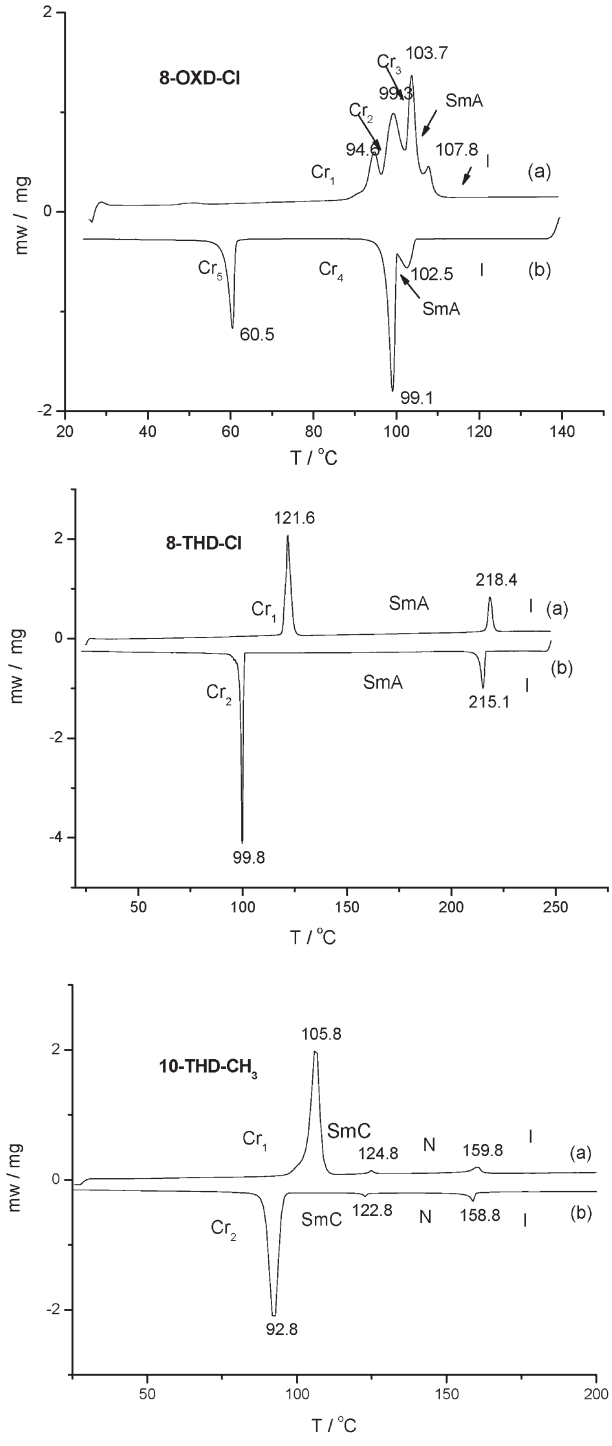

Figure 2. DSC curves of 8-OXD-Cl, 8-THD-Cl and 10-THD-CH3 on (a) heating and (b) cooling.

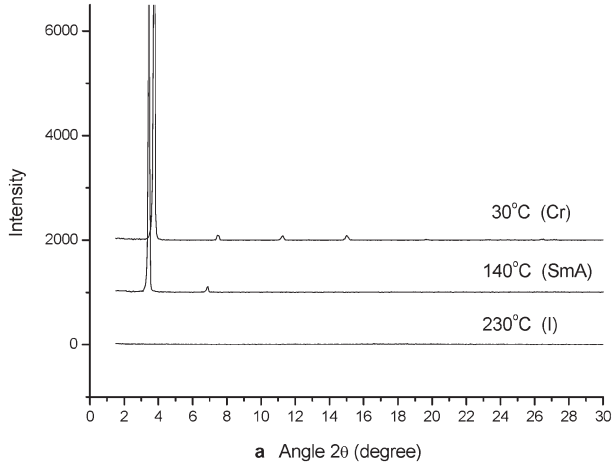

Figure 3. XRD patterns of 8-THD-Cl at different temperatures.

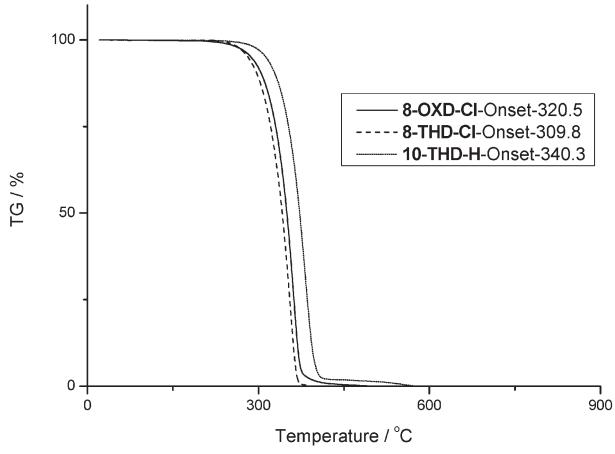

Figure 4. Thermogravimetric analysis curves of 8-OXD-Cl, 8-THD-Cl and 8-THD-H.

derivatives may reasonably explain the rich crystal-to-crystal transitions observed in ***n*-OXD-R**.

Recently, the effect of the terminal substituents on the liquid crystalline behaviour of heterocyclic liquid crystals has been studied by several research groups (*6b, 16*). The combined results show that the nature of mesophases of calamitic liquid crystals with electron-deficient core is mainly determined by the electronic factor of the terminal substituents. In this study, the 1,3,4-oxadiazole compound **10-OXD-Cl** exhibited an enantiotropic SmA phase, whereas the analogous compounds **10-OXD-H** and **10-OXD-CH$_3$** were non-mesogenic. The difference between liquid crystalline properties of is solely due to their different terminal groups. The electron-withdrawing chlorine atom may generate large dipole moment and secondary weak interactions, such as non-bonded C–H…Cl, both of which are helpful in stabilising the packing in the crystal and liquid crystal states (*17*). In contrast, the hydrogen atom and the electron-donating methyl group may not generate a large enough dipole moment to form a mesophase. As a consequence, the clearing points of these three compounds follow in the order: **10-OXD-Cl** (108.3°C) >**10-OXD-CH$_3$** (105.5°C)

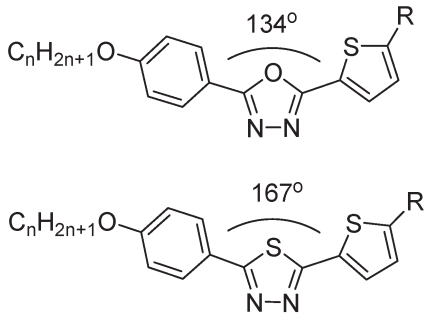

Scheme 2. The molecular structures of the 2,5-disubstituted 1,3,4-oxadiazoles and 1,3,4-thiazoles.

>**10-OXD-H** (95.4°C). As for the 1,3,4-thiadiazole derivatives **10-THD-Cl**, **10-THD-H** and **10-THD-CH_3**, their liquid crystal behaviors are also affected by the terminal groups. It is noted that formation of SmC and nematic phases in **10-THD-CH_3** is perhaps related to the dynamic nature of the freely-rotating methyl group.

Figure 5 shows the effect of the alkoxy chain length on the liquid crystal properties of ***n*-OXD-Cl**. The first three homologues exhibit no mesomorphic phase, whereas the others with n=8, 9, 10 exhibit an enantiotropic SmA phase and the mesomorphic temperature range tends to become wider with increasing alkoxy chain length. This trend in liquid crystal properties is commonly observed in calamitic mesogens (*18*). An increase in terminal length is often helpful to enhance dipole–dipole interaction between the terminal chains and facilitate the formation of a mesophase. In the case of ***n*-THD-Cl**, we found that the nature of the mesophase is not sensitive to the alkoxy length, all of the compounds ***n*-THD-Cl** exhibited an enantiotropic SmA phase. It is worth noting that the clearing points of this series of compounds follow a typical odd–even dependence on the length of alkoxy chain, as can be seen in Figure 6.

3. Experimental

General

4-Alkoxybenzoyl hydrazides **i**–**viii** were prepared by similar procedures (*19*). All the other chemicals and solvents were commercially available and used as received.

^{1}H NMR spectra were recorded using a Varain Mercury Plus 400 (400M) or Bruker AV300 (300 MHz) spectrometer with chemical shifts (in ppm) relative to tetramethylsilane. ^{13}C NMR spectra were recorded using the Bruker AV300 instrument (75 MHz). ESI-MS were recorded on a Finnigan LCQ Advantage spectrometer and high-resolution electron ionisation mass spectra (HRMS) were obtained with a Finnigan MAT 95 mass spectrometer.

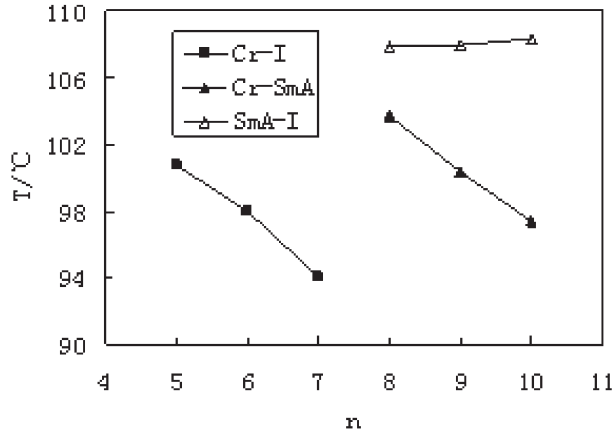

Figure 5. Plot of phase transition temperatures of ***n*-OXD-Cl** versus n.

The transition temperatures and enthalpies were investigated by a Netzsch DSC 204 differential scanning calorimeter at a heating and cooling rate of 5°C min^{-1} and calibrated with a pure indium sample. The optical textures were observed by POM using an Olympus BX51 equipped with a heating stage. Thermogravimetric analyses were performed using a Netzsch TG 209 instrument at a heating rate of 5°C min^{-1}. The variable-temperature X-ray diffractograms were recorded with a modular temperature chamber attachment (Material Research Instruments) in the temperature range 30–250°C at a reduced pressure (scan range=1.5–44° (2θ), step size=0.02°, scan time=1 s per step).

Synthesis of 5-substituted thienyl-2-carboxyl acid N′-(4-alkoxybenzoyl) hydrazides (i–viii)

Synthesis of **i**, chosen as an example to describe the general procedures, was as follows 5-Chloro-2-

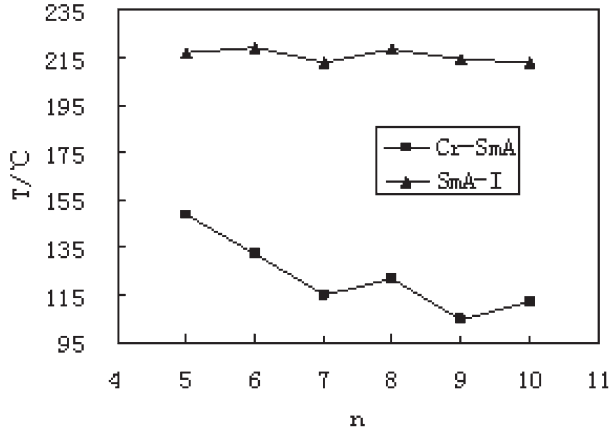

Figure 6. Plot of phase transition temperatures of ***n*-THD-Cl** versus n.

thiophenecarboxylic acid (700 mg, 4.3 mmol) and 10 ml of thionyl chloride were mixed and the solution refluxed for 4 h. Excess thionyl chloride was removed at reduced pressure to give the 5-chloro-2-thiophenecarbonyl chloride, which was added to a solution containing 4-pentyloxybenzoyl hydrazide (795.5 mg) in 30 ml of pyridine. The resultant reaction mixture was stirred for 8 h at room temperature and then heated to 90°C for 30 min. The reaction solution poured into 100 ml of cold water, and the resulting solid was filtered, washed several times with water and recrystallised from ethanol to afford 5-chlorothiophene-2-carboxyl acid *N*′-(4-hexyloxybenzoyl) hydrazide (**i**) as a white solid. Yield: 79%. ^{1}H NMR (300 MHz, $CDCl_3$): δ 0.94 (t, 3H, J=7.0 Hz), 1.36–1.48 (m, 4H), 1.81 (quintet, 2H), 4.00 (t, 2H, J=6.5 Hz), 6.89–6.93 (m, 3H, ArH and ThH), 7.52 (d, 1H, ThH, J=3.8 Hz), 7.81 (d, 2H, ArH, J=8.7 Hz), 9.15 (s, 1H), 9.74 (s, 1H). ESI-MS: m/z: 365.23 $[M-1]^-$.

For 5-chlorothiophene-2-carboxyl acid *N*′-(4-hexyloxybenzoyl) hydrazide (**ii**), yield: 81%, as white solid. ^{1}H NMR (300 MHz, $CDCl_3$): δ 0.90 (t, 3H, J=5.8 Hz), 1.34–1.49 (m, 6H), 1.80 (quintet, 2H), 4.00 (t, 2H, J=6.4 Hz), 6.88–6.93 (m, 3H, ArH and ThH), 7.51 (d, 1H, ThH, J=3.4 Hz), 7.82 (d, 2H, ArH, J=7.9 Hz), 9.18 (s, 1H), 9.93 (s, 1H). ESI-MS: m/z: 379.21 $[M-1]^-$.

For 5-chlorothiophene-2-carboxyl acid *N*′-(4-heptyloxybenzoyl) hydrazide (**iii**), yield: 90%, as white solid. ^{1}H NMR (400 MHz, $CDCl_3$): δ 0.90 (t, 3H, J=6.8 Hz), 1.33–1.50 (m, 8H), 1.81 (quintet, 2H), 4.00 (t, 2H, J=6.5 Hz), 6.88–6.94 (m, 3H, ArH and ThH), 7.52 (d, 1H, ThH, J=3.8 Hz), 7.81 (d, 2H, ArH, J=8.5 Hz), 9.16 (s, 1H), 9.90 (s, 1H). ESI-MS: m/z: 393.71 $[M-1]^-$.

For 5-chlorothiophene-2-carboxyl acid *N*′-(4-octyloxybenzoyl) hydrazide (**iv**), yield: 85%, as white solid. ^{1}H NMR (400 MHz, $CDCl_3$): δ 0.89 (t, 3H, J=6.0 Hz), 1.29–1.48 (m, 10H), 1.80 (quintet, 2H), 4.00 (t, 2H, J=6.5 Hz), 6.89–6.93 (m, 3H, ArH and ThH), 7.52 (d, 1H, ThH, J=3.4 Hz), 7.82 (d, 2H, ArH, J=8.3 Hz), 9.22 (s, 1H), 9.99 (s, 1H). ESI-MS: m/z: 407.28 $[M-1]^-$.

For 5-chlorothiophene-2-carboxyl acid *N*′-(4-nonyloxybenzoyl) hydrazide (**v**), yield: 82%, as white solid. ^{1}H NMR (400 MHz, $CDCl_3$): δ 0.88 (t, 3H, J=6.1 Hz), 1.28–1.45 (m, 12H), 1.79 (quintet, 2H), 3.97 (t, 2H, J=6.3 Hz), 6.86–6.91 (m, 3H, ArH and ThH), 7.52 (d, 1H, ThH, J=3.6 Hz), 7.80 (d, 2H, ArH, J=8.3 Hz), 9.20 (s, 1H), 9.97 (s, 1H). ESI-MS: m/z: 421.20 $[M-1]^-$.

For 5-chlorothiophene-2-carboxyl acid *N*′-(4-decanyloxybenzoyl) hydrazide (**vi**), yield: 88%, as white solid. ^{1}H NMR (400 MHz, $CDCl_3$): δ 0.88 (t, 3H, J=6.4 Hz), 1.28–1.48 (m, 14H), 1.81 (quintet, 2H), 4.02 (t, 2H, J=6.5 Hz), 6.89–6.94 (m, 3H, ArH and ThH), 7.52 (d, 1H, ThH, J=3.6 Hz), 7.81 (d, 2H, ArH, J=8.4 Hz), 9.18 (s, 1H), 9.93 (s, 1H). ESI-MS: m/z: 435.16 $[M-1]^-$.

For thiophene-2-carboxyl acid *N*′-(4-decanyloxybenzoyl) hydrazide (**vii**), yield: 87%, as white solid. ^{1}H NMR (300 MHz, $CDCl_3$): δ 0.87 (t, 3H, J=6.9 Hz), 1.22–1.47 (m, 14H), 1.79 (quintet, 2H), 3.99 (t, 2H, J=6.5 Hz), 6.87 (d, 2H, ArH, J=8.8 Hz), 7.06 (t, 1H, ThH, J=3.9 Hz), 7.49 (d, 1H, ThH, J=4.9 Hz), 7.75 (d, 1H, ThH, J=3.4 Hz), 7.81 (d, 2H, ArH, J=8.7 Hz), 9.45 (s, 1H), 9.61 (s, 1H). ESI-MS: m/z: 401.53 $[M-1]^-$.

For 5-methylthiophene-2-carboxyl acid *N*′-(4-decanyloxybenzoyl) hydrazide (**viii**), yield: 86%, as white solid. ^{1}H NMR (400 MHz, $CDCl_3$): δ 0.87 (t, 3H, J=6.9 Hz), 1.28–1.46 (m, 14H), 1.79 (quintet, 2H), 2.50 (s, 3H), 3.97 (t, 2H, J=6.5 Hz), 6.72 (d, 1H, ThH, J=2.8 Hz), 6.88 (d, 2H, ArH, J=8.4 Hz), 7.54 (d, 1H, ThH, J=3.3 Hz), 7.81 (d, 2H, ArH, J=8.5 Hz), 9.46 (s, 1H), 9.67 (s, 1H). ESI-MS: m/z: 415.55 $[M-1]^-$.

Synthesis of 2-(4-alkoxyphenyl)-5-(5-substituted thien-2-yl)-1,3,4-oxadiazoles (n-OXD-R)

This series of compounds was prepared according to general procedures as follows. The intermediate compound **i** (700 mg, 1.9 mmol) was added to 5 ml of thionyl chloride in anhydrous benzene (25 ml). The solution was refluxed for 7 h (TLC analysis revealed the completion of the reaction), and excess thionyl chloride and solvent were removed *in vacuo*. The crude solid was collected and washed several times with distilled water and was further purified by silica gel column chromatography using dichloromethane:ethyl acetate (v/v=25:1) as an eluent.

For 2-(4-pentyloxyphenyl)-5-(5-chlorothien-2-yl)-1,3,4-oxadiazole (**5-OXD-Cl**): yield 70%; m.p. 115.5°C. ^{1}H NMR (300 MHz, $CDCl_3$): δ 0.95 (t, 3H, J=7.2 Hz), 1.36–1.50 (m, 4H), 1.83 (quintet, 2H), 4.03 (t, 2H, J=6.6 Hz), 7.01 (d, 2H, ArH, J=8.7Hz; d, 1H, ThH, J=3.9 Hz), 7.58 (d, 1H, ThH, J=3.9 Hz), 8.01 (d, 2H, ArH, J=9.0 Hz). ^{13}C NMR (75 MHz, $CDCl_3$): δ 14.04, 22.49, 28.16, 28.82, 68.31, 115.03, 115.75, 124.03, 127.34, 128.60, 128.72, 135.06, 159.24, 162.10, 164.20. ESI-MS: m/z: 349.38 $[M+1]^+$. HRMS $[M+1]^+$: calculated for $C_{17}H_{17}ClN_2O_2S$, 349.0772; found, 349.0770.

For 2-(4-hexyloxyphenyl)-5-(5-chlorothien-2-yl)-1,3,4-oxadiazole (**6-OXD-Cl**): yield 76%; m.p. 98.0°C; white solid. ^{1}H NMR (300 MHz, $CDCl_3$): δ 0.92 (t, 3H, J=6.6 Hz), 1.35–1.51 (m, 6H), 1.82 (quintet, 2H), 4.03 (t, 2H, J=6.6 Hz), 7.00 (d, 2H,

ArH, J=8.7Hz; d, 1H, ThH, J=4.2 Hz), 7.57 (d, 1H, ThH, J=4.2 Hz), 8.01 (d, 2H, ArH, J=9.0 Hz). ^{13}C NMR (75 MHz, $CDCl_3$): δ 13.99, 22.57, 25.66, 29.10, 31.55, 68.33, 115.03, 115.69, 124.00, 127.32, 128.62, 128.69, 134.98, 159.24, 162.14, 164.13. ESI-MS: m/z: 363.36 $[M+1]^+$. HRMS $[M+1]^+$: calculated for $C_{18}H_{19}ClN_2O_2S$, 363.0928; found, 363.0927.

For 2-(4-heptyloxyphenyl)-5-(5-chlorothien-2-yl)-1,3,4-oxadiazole (**7-OXD-Cl**): yield 70%; m.p. 87.2°C; white solid. ^{1}H NMR (300 MHz, $CDCl_3$): δ 0.90 (t, 3H, J=6.6 Hz), 1.32–1.52 (m, 8H), 1.82 (quintet, 2H), 4.03 (t, 2H, J=6.6 Hz), 7.01 (d, 2H, ArH, J=8.9Hz; d, 1H, ThH, J=4.1 Hz), 7.58 (d, 1H, ThH, J=4.0 Hz), 8.01 (d, 2H, ArH, J=8.9 Hz). ^{13}C NMR (75 MHz, $CDCl_3$): δ 14.08, 22.61, 25.97, 29.04, 29.14, 31.77, 68.33, 115.03, 115.69, 123.99, 127.33, 128.65, 128.72, 135.01, 159.27, 162.14, 164.15. ESI-MS: m/z: 377.41 $[M+1]^+$. HRMS $[M+1]^+$: calculated for $C_{19}H_{21}ClN_2O_2S$, 377.1085; found, 377.1088.

For 2-(4-octyloxyphenyl)-5-(5-chlorothien-2-yl)-1,3,4-oxadiazole (**8-OXD-Cl**): yield 80%, as white solid. ^{1}H NMR (400 MHz, $CDCl_3$): δ 0.89 (t, 3H, J=7.0 Hz), 1.26–1.36 (m, 8H), 1.48 (quintet, 2H), 1.82 (quintet, 2H), 4.03 (t, 2H, J=6.5 Hz), 7.01 (d, 2H, ArH, J=8.4Hz; d, 1H, ThH, J=4.9 Hz), 7.58 (d, 1H, ThH, J=4.0 Hz), 8.01 (d, 2H, ArH, J=8.7 Hz). ^{13}C NMR (75 MHz, $CDCl_3$): δ 14.11, 22.69, 26.09, 29.17, 29.25, 29.41, 31.84, 68.39, 115.13, 115.76, 124.05, 127.40, 128.67, 128.79, 135.06, 159.35, 162.20, 164.24. ESI-MS: m/z: 391.38 $[M+1]^+$. HRMS $[M+1]^+$: calculated for $C_{20}H_{23}ClN_2O_2S$, 391.1241; found, 391.1245.

For 2-(4-nonyloxyphenyl)-5-(5-chlorothien-2-yl)-1,3,4-oxadiazole (**9-OXD-Cl**): yield 78%, as white solid. ^{1}H NMR (400 MHz, $CDCl_3$): δ 0.89 (t, 3H, J=6.6 Hz), 1.25–1.36 (m, 10H), 1.48 (quintet, 2H), 1.82 (quintet, 2H), 4.03 (t, 2H, J=6.6 Hz), 7.01 (d, 2H, ArH, J=8.6Hz; d, 1H, ThH, J=4.1 Hz), 7.58 (d, 1H, ThH, J=4.0 Hz), 8.02 (d, 2H, ArH, J=8.8 Hz). ^{13}C NMR (75 MHz, $CDCl_3$): δ 14.10, 22.67, 26.00, 29.14, 29.25, 29.38, 29.52, 31.88, 68.34, 115.03, 115.70, 124.00, 127.33, 128.64, 128.72, 135.02, 159.28, 162.14, 164.16. ESI-MS: m/z: 405.49 $[M+1]^+$. HRMS $[M+1]^+$: calculated for $C_{21}H_{25}ClN_2O_2S$, 405.1398; found, 405.1395.

For 2-(4-decyloxyphenyl)-5-(5-chlorothien-2-yl)-1,3,4-oxadiazole (**10-OXD-Cl**): yield 75%, as white solid. ^{1}H NMR (400 MHz, $CDCl_3$): δ 0.89 (t, 3H, J=6.6 Hz), 1.28–1.36 (m, 12H), 1.48 (quintet, 2H), 1.82 (quintet, 2H), 4.03 (t, 2H, J=6.5 Hz), 7.00-7.02 (m, 3H, ArH and ThH), 7.58 (d, 1H, ThH, J=4.0 Hz), 8.01 (d, 2H, ArH, J=8.7 Hz). ^{13}C NMR (75 MHz, $CDCl_3$): δ 14.11, 22.69, 26.01, 29.14, 29.32, 29.38, 29.56, 31.90, 68.35, 115.05, 115.72, 124.01, 127.33, 128.65, 128.74, 135.04, 159.30, 162.15, 164.18. ESI-MS: m/z: 419.45 $[M+1]^+$. HRMS $[M+1]^+$: calculated for $C_{22}H_{27}ClN_2O_2S$, 419.1555; found, 419.1548.

For 2-(4-decyloxyphenyl)-5-(thien-2-yl)-1,3,4-oxadiazole (**10-OXD-H**): yield 71%; m.p. 95.4°C; white solid. ^{1}H NMR (400 MHz, $CDCl_3$): δ 0.88 (t, 3H, J=6.8 Hz), 1.28–1.36 (m, 12H), 1.48 (quintet, 2H), 1.82 (quintet, 2H), 4.02 (t, 2H, J=6.6 Hz), 7.01 (d, 2H, ArH, J=8.5 Hz), 7.19 (t, 1H, ThH, J=4.3 Hz), 7.56 (d, 1H, ThH, J=4.9 Hz), 7.82 (d, 1H, ThH, J=3.3 Hz), 8.04 (d, 2H, ArH, J=8.5 Hz). ^{13}C NMR (75 MHz, $CDCl_3$): δ 14.08, 22.66, 25.99, 29.13, 29.30, 29.36, 29.54, 31.88, 68.30, 114.99, 115.93, 125.50, 128.08, 128.68, 129.40, 129.76, 160.35, 162.03, 164.06. ESI-MS: m/z: 791.15 $[2M+Na]^+$. HRMS $[M+1]^+$: calculated for $C_{22}H_{27}ClN_2O_2S$, 385.1944; found, 385.1952.

For 2-(4-decyloxyphenyl)-5-(5-methlthien-2-yl)-1,3,4-oxadiazole (**10-OXD-CH$_3$**): yield 77%; m.p. 105.5°C; white solid. ^{1}H NMR (400 MHz, $CDCl_3$): δ 0.88 (t, 3H, J=7.0 Hz), 1.28–1.38 (m, 12H), 1.47 (quintet, 2H), 1.82 (quintet, 2H), 2.57 (s, 3H), 4.02 (t, 2H, J=6.6 Hz), 6.84 (d, 1H, ThH, J=3.6 Hz), 7.00 (d, 2H, ArH, J=8.8 Hz), 7.60 (d, 1H, ThH, J=3.6 Hz), 8.02 (d, 2H, ArH, J=8.8 Hz). ^{13}C NMR (75 MHz, $CDCl_3$): δ 14.07, 15.44, 22.65, 25.99, 29.13, 29.29, 29.36, 29.54, 31.88, 68.28, 114.94, 116.06, 122.94, 126.48, 128.57, 129.62, 145.22, 160.31, 161.90, 163.74. ESI-MS: m/z: 399.49 $[M+1]^+$. HRMS $[M+1]^+$: calculated for $C_{22}H_{27}ClN_2O_2S$, 399.2101; found, 399.2106.

Synthesis of 2-(4-alkoxyphenyl)-5-(5-substituted thien-2-yl)-1,3,4-thiadiazoles (n-THD-R)

Compounds ***n*-THD-Cl** (n=5–8) were prepared under microwave irradiation and solvent-free conditions. The synthesis of **5-THD-Cl** is taken as an example to describe the procedures. The intermediate **i** (367 mg, 1 mmol) and 444 mg (1.1 mmol) Lawesson's reagent (p-methoxyphenylthionophosphine sulfide dimer) were mixed and then irradiated in a microwave oven (800 W) for 120 s. After cooling to room temperature, the reaction mixture was removed from the oven and dissolved in 3 ml of dichloromethane. The crude product was purified by column chromatography [silica gel/dichloromethane:ethyl acetate, v/v=25:1] to afford 2-(4-pentyloxyphenyl)-5-(5-chlorothien-2-yl)-1,3,4-thiadiazole (**5-THD-Cl**). Yield: 36%, as pale yellow solid. ^{1}H NMR (400 MHz, $CDCl_3$): δ 0.95 (t, 3H, J=7.2 Hz), 1.37–1.46 (m, 4H), 1.82 (quintet, 2H), 4.02 (t, 2H, J=6.6 Hz), 6.95 (d, 1H, ThH, J=4.0 Hz), 6.97 (d, 2H, ArH, J=8.8 Hz), 7.29 (d, 1H, ThH, J=4.0 Hz), 7.88 (d, 2H, ArH, J=8.8 Hz). ^{13}C NMR (75 MHz, $CDCl_3$): δ 14.00, 22.45, 28.15, 28.84, 68.30, 115.09, 122.20, 127.08, 128.38, 129.47, 131.30, 134.21,

160.06, 161.72, 167.36. ESI-MS: m/z: 365.27 $[M+1]^+$. HRMS $[M+1]^+$: calculated for $C_{17}H_{17}ClN_2OS_2$, 365.0544; found, 365.0540.

For 2-(4-hexyloxyphenyl)-5-(5-chlorothien-2-yl)-1,3,4-thiadiazole (**6-THD-Cl**), yield: 32%, as pale yellow solid. ^{1}H NMR (300 MHz, $CDCl_3$): δ 0.92 (t, 3H, J=6.9 Hz), 1.32–1.39 (m, 4H), 1.48 (quintet, 2H), 1.82 (quintet, 2H), 4.02 (t, 2H, J=6.6 Hz), 6.95–6.99 (m, 3H, ThH and ArH), 7.30 (d, 1H, ThH, J=4.0 Hz), 7.89 (d, 2H, ArH, J=8.8 Hz). ^{13}C NMR (75 MHz, $CDCl_3$): δ 14.04, 22.61, 25.69, 29.12, 31.57, 68.33, 115.10, 122.19, 127.08, 128.40, 129.49, 131.30, 134.23, 160.09, 161.73, 167.37. ESI-MS: m/z: 379.35 $[M+1]^+$. HRMS $[M+1]^+$: calculated for $C_{18}H_{19}ClN_2OS_2$, 379.0700; found, 379.0696.

For 2-(4-heptyloxyphenyl)-5-(5-chlorothien-2-yl)-1,3,4-thiadiazole (**7-THD-Cl**), yield: 25%, as pale yellow solid. ^{1}H NMR (300 MHz, $CDCl_3$): δ 0.90 (t, 3H, J=6.8 Hz), 1.32–1.50 (m, 8H), 1.82 (quintet, 2H), 4.02 (t, 2H, J=6.6 Hz), 6.95–6.99 (m, 3H, ThH and ArH), 7.30 (d, 1H, ThH, J=4.0 Hz), 7.89 (d, 2H, ArH, J=8.8 Hz). ^{13}C NMR (75 MHz, $CDCl_3$): δ 14.08, 22.61, 25.97, 29.05, 29.16, 31.77, 68.33, 115.11, 122.20, 127.07, 128.37, 129.49, 131.32, 134.23, 160.08, 161.73, 167.37. ESI-MS: m/z: 393.38 $[M+1]^+$. HRMS $[M+1]^+$: calculated for $C_{19}H_{21}ClN_2OS_2$, 393.0857; found, 393.0858.

For 2-(4-octyloxyphenyl)-5-(5-chlorothien-2-yl)-1,3,4-thiadiazole (**8-THD-Cl**), yield: 50%, as pale yellow solid. ^{1}H NMR (400 MHz, $CDCl_3$): δ 0.89 (t, 3H, J=6.5 Hz), 1.30–1.48 (m, 10H), 1.82 (quintet, 2H), 4.03 (t, 2H, J=6.4 Hz), 6.99–7.01 (m, 3H, ThH and ArH), 7.57 (d, 1H, ThH, J=3.9 Hz), 8.01 (d, 2H, ArH, J=8.6 Hz). ^{13}C NMR (75 MHz, $CDCl_3$): δ 14.06, 22.64, 26.00, 29.15, 29.21, 29.33, 31.80, 68.35, 115.13, 122.23, 127.06, 128.34, 129.49, 131.33, 134.24, 160.06, 161.75, 167.36. ESI-MS: m/z: 407.35 $[M+1]^+$. HRMS $[M+1]^+$: calculated for $C_{20}H_{23}ClN_2OS_2$, 407.1013; found, 407.1013.

Compounds **9-THD-Cl** and **10-THD-R** (R=Cl, H, CH_3) were prepared according to the following procedures. Lawesson's reagent (444 mg, 1.1 mmol) was added to a solution of the respective intermediate **v**–**viii** (1 mmol) in anhydrous toluene. The reaction mixture was heated under reflux while stirring for 10 h (TLC analysis revealed the completion of the reaction), then the crude product was obtained by removing the solvent *in vacuo* and purifying by column chromatography [silica gel/dichloromethane:ethyl acetate, v/v=25:1] to afford a pale yellow solid.

For 2-(4-nonyloxyphenyl)-5-(5-chlorothien-2-yl)-1,3,4-thiadiazole (**9-THD-Cl**), yield: 62%, as pale yellow solid. ^{1}H NMR (400 MHz, $CDCl_3$): δ 0.89 (t, 3H, J=6.7 Hz), 1.29–1.51 (m, 12H), 1.82 (quintet, 2H), 4.02 (t, 2H, J=6.5 Hz), 6.96–6.99 (m, 3H, ThH and ArH), 7.32 (d, 1H, ThH, J=3.5 Hz), 7.90 (d, 2H, ArH, J=8.5 Hz). ^{13}C NMR (75 MHz, $CDCl_3$): δ 14.09, 22.67, 26.00, 29.15, 29.25, 29.38, 29.52, 31.88, 68.34, 115.12, 122.21, 127.06, 128.36, 129.49, 131.32, 134.24, 160.18, 161.74, 167.36. ESI-MS: m/z: 421.40 $[M+1]^+$. HRMS $[M+1]^+$: calculated for $C_{21}H_{25}ClN_2OS_2$, 421.1170; found, 421.1175.

For 2-(4-decyloxyphenyl)-5-(5-chlorothien-2-yl)-1,3,4-thiadiazole (**10-THD-Cl**), yield: 65%, as pale yellow solid. ^{1}H NMR (400 MHz, $CDCl_3$): δ 0.89 (t, 3H, J=7.1 Hz), 1.28–1.50 (m, 14H), 1.81 (quintet, 2H), 4.02 (t, 2H, J=6.6 Hz), 6.95 (d, 1H, ThH, J=4.0 Hz), 6.98 (d, 2H, ArH, J=8.8 Hz), 7.30 (d, 1H, ThH, J=4.0 Hz), 7.89 (d, 2H, ArH, J=8.8 Hz). ^{13}C NMR (75 MHz, $CDCl_3$): δ 14.10, 22.68, 26.00, 29.14, 29.32, 29.37, 29.56, 31.90, 68.35, 115.13, 122.23, 127.07, 128.36, 129.50, 131.32, 134.26, 160.09, 161.74, 167.37. ESI-MS: m/z: 435.33 $[M+1]^+$. HRMS $[M+1]^+$: calculated for $C_{22}H_{27}ClN_2OS_2$, 435.1326; found, 435.1323.

For 2-(4-decyloxyphenyl)-5-(thien-2-yl)-1,3,4-thiadiazole (**10-THD-H**), yield: 68%, as white solid. ^{1}H NMR (400 MHz, $CDCl_3$): δ 0.88 (t, 3H, J=6.8 Hz), 1.28–1.35 (m, 12H), 1.46 (quintet, 2H), 1.81 (quintet, 2H), 4.00 (t, 2H, J=6.5 Hz), 6.97 (d, 2H, ArH, J=8.5 Hz), 7.13 (t, 1H,ThH, J=4.2 Hz), 7.48 (d, 1H, ThH, J=4.8 Hz), 7.55 (d, 1H, ArH, J=3.1 Hz), 7.90 (d, 2H, ArH, J=8.4 Hz). ^{13}C NMR (75 MHz, $CDCl_3$): δ 14.09, 22.67, 26.00, 29.15, 29.31, 29.37, 29.55, 31.89, 68.30, 115.07, 122.42, 127.91, 128.97, 129.22, 129.43, 132.72, 160.92, 161.60, 167.25. ESI-MS: m/z: 401.30 $[M+1]^+$. HRMS $[M+1]^+$: calculated for $C_{22}H_{27}ClN_2O_2S$, 401.1716; found, 401.1723.

For 2-(4-decyloxyphenyl)-5-(5-methlthien-2-yl)-1,3,4-thiadiazole (**10-THD-CH$_3$**), yield: 72%, as pale yellow solid. ^{1}H NMR (400 MHz, $CDCl_3$): δ 0.88 (t, 3H, J=7.1 Hz), 1.28–1.37 (m, 12H), 1.46 (quintet, 2H), 1.81 (quintet, 2H), 2.54 (s, 3H), 4.00 (t, 2H, J=6.5 Hz), 6.78 (d, 1H, ThH, J=3.6 Hz), 6.97 (d, 2H, ArH, J=8.7 Hz), 7.35 (d, 1H, ThH, J=3.6 Hz), 7.88 (d, 2H, ArH, J=8.7 Hz). ^{13}C NMR (75 MHz, $CDCl_3$): δ 14.10, 15.50, 22.68, 26.01, 29.17, 29.32, 29.40, 29.57, 31.90, 68.26, 114.99, 122.50, 126.31, 129.32, 129.49, 130.23, 144.29, 161.12, 161.47, 166.66. ESI-MS: m/z: 415.58 $[M+1]^+$. HRMS $[M+1]^+$: calculated for $C_{22}H_{27}ClN_2OS_2$, 415.1872; found, 415.1877.

4. Conclusion

Two new series of heterocyclic mesomorphic compounds containing 1,3,4-oxadiazole/1,3,4-thiadiazole and thiophene rings were synthesised and characterised. The 1,3,4-thiadiazole compounds are more

helpful in forming stable mesophases with wide mesomorphic temperature ranges than the corresponding 1,3,4-oxadiazole derivatives. The nature of the mesophase was influenced by the electronic properties of the terminal groups; electron-withdrawing chlorine tends to form a smectic A phase, whereas electron-donating methyl facilitates nematic and smectic C phases. The clearing points of 1,3,4-thiadiazole compounds were found to follow a typical odd–even alternation with increasing alkoxy chain length.

Acknowledgements

This work was financially supported by grants from the National Natural Science Foundation of China (Project No. 20772064). We thank for Dr. Stephen Chui and Prof. Chi-Ming Che (Department of Chemistry, The University of Hong Kong) for assistance in the VXRD measurements.

References

(1) (a) Gray G.W. *Thermotropic Liquid Crystals;* John Wiley: 1987; (b) Narasimhaswamy, T.; Somanathan, N.; Ramamoorthy, A. *Chem. Mater*. **2005**, *17*, 2013–2018.

(2) Kumar S. *Liquid Crystals, Experimental Study of Physical Properties and Phase Transitions*; Cambridge University Press: Cambridge, 2001. pp. p 397.

(3) (a) Lai C.K.; Liu H.C.; Li F.J.; Cheng K.L.; Sheu H.S. *Liq. Cryst.* **2005**, *32*, 85–94; (b) Su, C.; Lee, L.X.; Yu, S.-H. *Liq. Cryst*. **2004**, *31*, 745–749; (c) Parra, M.L.; Saavedra, C.G.; Hidalgo, P.I.; Elgueta, E.Y. *Liq. Cryst*. **2008**, *35*, 55–64.

(4) Wu L.H.; Wang Y.C.; Hsu C.S. *Liq. Cryst.* **2000**, *27*, 1503–1513.

(5) (a) Mochizuki H.; Hasui Y.; Kawamoto M.; Shiono T.; Ikeda T.; Adachi C.; Taniguchi Y.; Shirota Y. *Chem. Commun.* **2000**, 1923–1924; (b) Hughes, G.; Kreher, D.; Wang, C.; Batsanov, A.S.; Bryce, M.R. *Org. Biomol. Chem*. **2004**, *2*, 3363–3367; (c) Kang, S.; Saito, Y.; Watanabe, N.; Tokita, M.; Takanishi, Y.; Takezoe, H.; Watanabe, J. *J. Phys. Chem. B* **2006**, *110*, 5205–5214.

(6) (a) Kamtekar K.T.; Wang C.; Bettington S.; Batsanov A.S.; Perepichka I.F.; Bryce M.R.; Ahan J.H.; Rabinal M.; Petty M.C. *J. Mater. Chem.* **2006**, *16*, 3823–3835; (b) Han, J.; Chui, S.S.Y.; Che, C.M. *Chem. Asian J*. **2006**, *1*, 814–825.

(7) (a) Han J.; Wang Y.M.; Wang X.G. *Chin. J. Chem.* **2006**, *24*, 1594–1598; (b) Kimura, M.; Yasuda, T.; Kishimoto, K.; Götz, G.; Bäuerle, P.; Kato, T. *Chem. Lett*. **2006**, *35*, 1150–1151; (c) Parakos, A.J.; Swager, T.M. *Chem. Mater*. **2002**, *14*, 4543–4549.

(8) (a) Goddart C.J. *J. Heterocylic Chem.* **1991**, *28*, 17–28; (b) Tully, W.G.; Gardner, C.R.; Gillepie, R.J.; Westwood, W. *J. Med. Chem*. **1991**, *34*, 2060–2067; (c) Perez, M.; Bermejo, J. *J. Org. Chem*. **1993**, *58*, 2628–2630; (d) Wang, Y.; Sauer, D.R.; Djuric, S.W. *Tetrahedron Lett*. **2006**, *47*, 105–108.

(9) (a) Thomsen I.; Pedersen U.; Rasmussen P.B.; Yde B.; Andersen T.P.; Lawesson S.O. *Chem. Lett.* **1983**, 809–810; (b) Sybo, B.; Bradley, P.; Grubb, A.; Miller, S.; Proctor K.J.; Clowes, W.L.; Laawrie, M.R.; Sampson, P.; Seed, A.J. *J. Mater. Chem*. **2007**, 17, 3406–3411; (c) Jesberger, M.; Davis, T.P.; Barner, L. *Synthesis*, **2003**, *13*, 1929–1958.

(10) (a) Kiryanov A.A.; Sampson P.; Seed A.J. *J. Org. Chem.* **2001**, *66*, 7925–7929; (b) Huang, H.; Yu, H.; Chen, P.; Han, J.; Meng, J. *Chin. J. Org. Chem*. **2004**, *24*, 502–505.

(11) Kumar S. *Liquid Crystals: Experimental Study of Physical Properties and Phase Transition*; Cambridge University Press: Cambridge, 2001. pp. pp 1–65.

(12) Dierking I. *Texture of Liquid Crystals*; Wiley-VCH Verlag: Weinheim, 2003.

(13) (a) Collings P.J.; Hird M., In *Introduction to Liquid Crystals*; Gray G.W., Goodby J.W., Fukuda A., Eds.; Taylor & Francis: London, 1997; p 192; (b) Deun, R.V.; Parac-Vogt, T.N.; Hecke, K.V.; Meervelt, L.V.; Binnemans, K.; Guillon, D.; Donnio, B. *J. Mater. Chem*. **2003**, *13*, 1639–1645; (c) Zhang, P.; Qu, S.N.; Wang, H.T.; Bai, B.L.; Li, M. *Liq. Cryst*. **2008**, *35*, 389–394.

(14) (a) Wang C.; Batsanov A.S.; Bryce M.R. *Chem. Commun.* **2004**, 578–579; (b) Yu, H.T.; Huang, Y.D.; Meng, J.B.; Wang, Y.M. *Chin. J. Struct. Chem*. **2002**, *21*, 153–156; (c) Huang, H.M.; Yu, H.T.; Chen, P.L.; Meng, J.B. *Acta crystallogr. E* **2004**, *60*, o881–o883; (d) Liao, C.T.; Wang, Y.J.; Huang, C.S.; Sheu, H.S.; Lee, G.H.; Lai, C.K. *Tetrahedron* **2007**, *63*, 12437–12445; (e) Seed, A. *Chem. Soc. Rev*. **2007**, *36*, 2046–2069.

(15) Parra M.; Hernández S.; Alderete J.; Zúñiga C. *Liq. Cryst.* **2000**, *27*, 995–1000.

(16) (a) Wang C.S.; Wang I.W.; Cheng K.L.; Lai C.K. *Tetrahedron* **2006**, *62*, 9383–9392; (b) Sung, H.H.; Lin, H.C. *Liq. Cryst*. **2004**, *31*, 831–841.

(17) Dunitz J.D.; Schweizer W.B. *Chem. Eur. J.* **2006**, *12*, 6804–6815.

(18) Chai C.P.; Yang Q.; Fan X.H.; Chen X.F.; Shen Z.H.; Zhou Q.F. *Liq. Cryst.* **2008**, *35*, 133–141.

(19) (a) Sybo B.; Bradley P.; Grubb A.; Miller S.; Proctor K.J.W.; Clowes L.; Lawrie M.R.; Sampson P.; Seed A.J. *J. Mater. Chem.* **2007**, *17*, 3406–3411; (b) Zhang, X.B.; Tang, B.C.; Zhang, P.; Li, M.; Tian, W.J. *J. Mol. Struct*. **2007**, *846*, 55–64.